

Article

Permeability Enhancement Mechanism of Acidizing in Steam-Assisted Gravity Flooding Wells

Ming Yu ¹, Chao Xu ², Yujie Bai ³, Che Zou ³, Weibo Liu ³, Guangsheng Cao ^{3,*}, Xi Yi ³ and Jing Zhang ⁴

¹ Institute of Geology, No. 6 Oil Production Plant, Daqing Oilfield Co., Ltd., Daqing 163114, China; yuming03@petrochina.com.cn

² Petrochina Xinjiang Oilfield Branch, Production Operations Department, Karamay 834000, China; fcxuc1@petrochina.com.cn

³ Key Laboratory of Enhanced Oil Recovery, Ministry of Education, College of Petroleum Engineering, Northeast Petroleum University, Daqing 163318, China; sygcbj@163.com (Y.B.); zc20180902@163.com (C.Z.); 15765966880@163.com (W.L.); vickyyx@163.com (X.Y.)

⁴ Institute of Geology, No. 1 Oil Production Plant, Daqing Oilfield Co., Ltd., Daqing 163453, China; zhang15@petrochina.com

* Correspondence: nepucgswz@163.com

Abstract: Steam-assisted gravity oil drainage (SAGD flooding) is a cutting-edge technology for the development of oils which is gradually replacing steam huff and puff and is being used more and more widely. Low-permeability interlayers are generally developed in oil reservoirs in China, which may shield the migration of steam, oil and gas. Targeted acidizing fracturing was proposed to break through the low-permeability interlayers, and hence, the problem that the hindrance to the expansion of the steam chamber led to heat loss and seriously affected the development effect could be solved. A typical kind of well with SAGD flooding actually applied in China, Shuyi District of Liaohe Oilfield, was taken as the example for studying the optimization of crack parameters. Based on the study of reservoir sensitivity characteristics in this well, the formulations of working fluids for targeted acidizing fracturing were developed by optimizing the weight percentages of main acid solution and additives. The formula of ‘4% hydrochloric acid + 2% polyphosphoric acid + 5% fluoroboric acid + 4% acetic acid’ could be used as the acidizing fracturing working fluid for typical blocks of the Shuyi District of Liaohe Oilfield, which can increase the permeability of the natural core by 40.19–57.06%. Studies on targeted acidizing fracturing are beneficial for enhancing the oil recovery of oil reservoirs.

Keywords: steam-assisted gravity drive; enhanced oil recovery; acidification; low-permeability intervals; increased permeability



Citation: Yu, M.; Xu, C.; Bai, Y.; Zou, C.; Liu, W.; Cao, G.; Yi, X.; Zhang, J. Permeability Enhancement Mechanism of Acidizing in Steam-Assisted Gravity Flooding Wells. *Processes* **2023**, *11*, 3004. <https://doi.org/10.3390/pr11103004>

Academic Editors: Luigi Piga, Jan Vinogradov, Ali Habibi and Zhengyuan Luo

Received: 25 August 2023

Revised: 12 October 2023

Accepted: 16 October 2023

Published: 19 October 2023



Copyright: © 2023 by the authors. Licensee MDPI, Basel, Switzerland. This article is an open access article distributed under the terms and conditions of the Creative Commons Attribution (CC BY) license (<https://creativecommons.org/licenses/by/4.0/>).

1. Introduction

Steam-assisted gravity oil drainage technology, abbreviated as SAGD, is a cutting-edge technology for developing oil by using steam as a heat source [1]. During the SAGD process, the convection between oil, water and steam is realized through the combination of heat conduction and heat convection, and crude oil can be produced by relying on the gravity of crude oil and condensate [2,3]. The theory of SAGD was proposed by Canadian scholar Butler in 1979 [4]. The basic principle is that steam is continuously injected into the formation through a horizontal well located above the horizontal production well. The steam pressure is maintained, and the steam gradually diffuses above the well to form an inverted triangular-shaped steam chamber. The surrounding area of the chamber wall is relatively cold oil sands, where steam diffuses to the interface and condenses [5]. The released heat is transmitted to the surrounding area, causing the crude oil near the interface to be heated. Under the action of gravity, the heated crude oil flows down to the production well below, while the continuous production of crude oil with reduced viscosity further promotes the outward expansion of the steam chamber. In 1981, Butler [6]

assumed that the oil leakage process expands from the original theoretical two-dimensional direction to a three-dimensional direction. The oil leakage rate in the new hypothesis is taken as an important variable to derive an equation where the relationship is expressed. In 1986, the Alberta Oil Sands Technology and Research Authority used the SAGD equation proposed by Butler to launch the world's first SAGD pilot experimental project, namely, the Underground Test Facilities (UFT) project [7]. The UFT project achieved great success in pilot production, proving that SAGD technology is suitable for oil recovery. In 1996, Canada launched its first commercial SAGD project (Cenovus Foster Creek project), which reached its peak production in 2014 [8,9]. By the end of 2015, Canada completed 26 commercial development projects with an annual oil production of over 5000×10^4 t, accounting for approximately 42% of Canadian total oil sand production. In 1999, Y. Ito [10] studied the flow patterns of steam, water and oil during the SAGD process, as well as the heat transfer mechanism of steam to crude oil. The research results indicate that the main heat transfer mechanism of the SAGD process is thermal convection, rather than heat conduction as previously proposed by Butler. The flow when the steam chamber rises is different from the conventional flow during lateral expansion. At the top of the steam chamber, the lighter steam is located below the oil, making the interface unstable and prone to fingering. This theory was initially proposed by Butler, and the steam fingering phenomenon was explained for the first time using on-site measured data by Y. Ito in a piece of literature published in 2005 [11]. I.D. Gates [12,13] studied steam injection optimization methods for reservoirs with gas caps in 2006. A higher initial injection rate and pressure should be used to make the steam chamber come in contact with the gas cap and then reduce the injection rate to balance the pressure of the top gas, thereby avoiding or reducing convective heat loss caused by steam in the gas cap area. In addition, the decrease in steam chamber pressure also reduces heat conduction losses on the overlying and underlying rock layers. However, it should be noted that a decrease in steam chamber pressure can also lead to a decrease in temperature and an increase in the viscosity of oil. In 2010, Sharma [14] deduced a new model for the gravity drainage of super oil flowing at the edge of a steam chamber. The location where the maximum oil velocity occurs depends on the curvature of oil relative permeability curve to water and the oil viscosity. In the verification with the actual situation on-site, it is shown that the relative permeability effect is an indispensable part when calculating the actual oil production rate [15,16]. In reservoirs that have already been developed using the SAGD method, it has been found that some well groups have problems such as poor connectivity between the injection well and production well, high water cut and low production during the SAGD development process [17]. These phenomena can be explained in that the presence of intervals with low physical properties in the reservoir hinders the expansion of the steam chamber and makes it difficult to form effective drainage channels [18]. A large amount of research and on-site experience have shown that there will be pieces of remaining oil above the intervals when the intervals with low physical properties existing above the steam injection well are continuously difficult to be broken through, as demonstrated in Figure 1. Due to the shallow depth of the actual formation in Liaohe Oilfield, the fracture morphology is mainly horizontal fractures. Therefore, acid gas can be used to dissolve the upper part of the acid-corroded fractures. Therefore, the acid-corroded fractures are perpendicular to the formation and can dissolve upwards or downwards, communicating different layers [19–21]. When the intervals with low physical properties exist between the steam injection well and the production well, as shown in Figure 2, they may severely limit the recovery rate by blocking the flow of crude oil whose viscosity is reduced by heat towards the production well [22]. In order to continuously improve the development effect of the SAGD method and achieve economic and effective development of SAGD flooding, there are still large spaces for technological improvement in areas such as breaking through the intervals with low physical properties as soon as possible, continuously expanding the swept volume of the steam chamber, increasing crack conductivity and improving supporting processes.

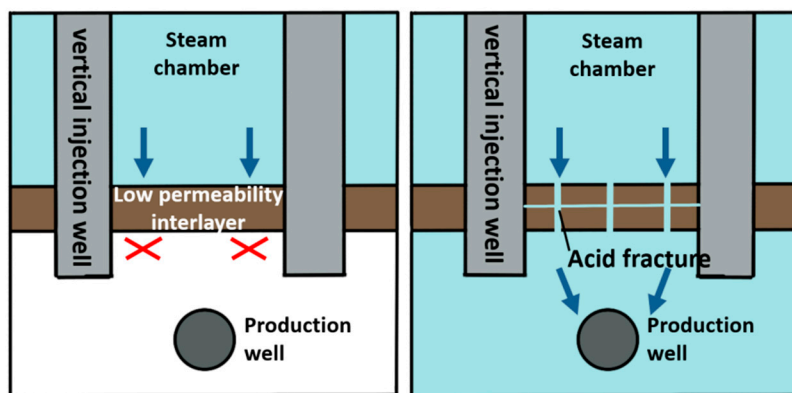


Figure 1. Application schematic diagram of acidizing fracturing in the intervals with low physical properties above the steam injection well.

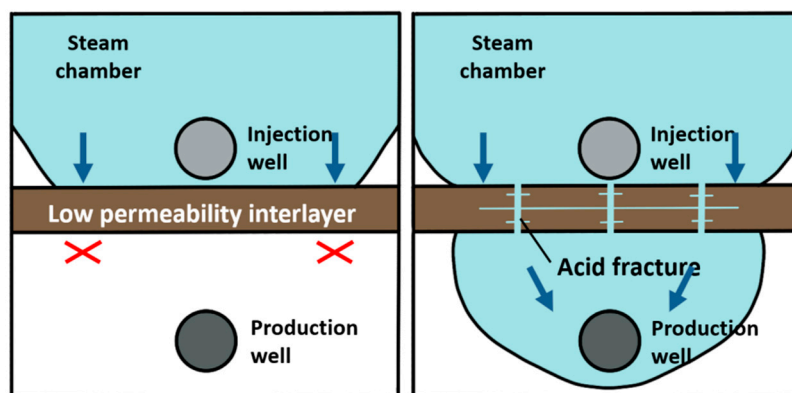


Figure 2. Application schematic diagram of acidizing fracturing in the intervals with low physical properties between steam injection well and production well.

Acidizing fracturing, which refers to the injection of acid into the formation under conditions where the acid injection pressure at the bottom of the well is greater than the fracturing pressure of the formation rock, is a commonly used stimulation method in oil fields. The formation is fractured to form artificial cracks, and the acid always flows in the open cracks and reacts with the fracture wall. Fractures with a certain length and acid corrosion conductivity are ultimately formed to improve the seepage capacity of the reservoir, thus enhancing permeability [23]. In the early stage, all studies on SAGD processes were conducted based on homogeneous reservoir models. In 1992, Yang and Butler [24,25] conducted physical experiments simulating heterogeneous reservoirs. Two representative on-site conditions of shale interlayers in the reservoir and horizontal layers with different permeability in the reservoir were simulated using a two-dimensional sand-packed model. During the experiment, a two-dimensional model filled with micron glass beads was used as the porous medium and reinforced phenolic resin partitions were used to simulate shale interlayers. Thermocouples were inserted into the production well to record well temperature data. By changing the position and direction of the interlayer, 10 different situations were studied. It can be concluded from the experiments that relatively short interlayers have little impact on overall performance, while the presence of long thin interlayers can result in reduced production. For situations where there is a longer interlayer, when the steam chamber expands laterally, the asphalt above the interlayer is also heated by the heat conduction of the interlayer. However, due to the barrier effect of the interlayer, the asphalt may not flow to the production well. The addition of nitrogen in the steam injection process is helpful for extracting asphalt above the interlayer. By reasonably arranging the positions of steam injection wells and production wells, the influence of horizontal or inclined interlayers on oil recovery can be overcome. Understanding the conditions of the interlayer in the reservoir can facilitate a better design of the SAGD

project. In 1995, Kisman [26] conducted a numerical simulation study on the SAGD effect of the Burnt Lake reservoir located in northeastern Alberta, Canada. Based on reservoir properties such as permeability, relative permeability, wettability, viscosity, thermophysical properties and positions of interlayers, a two-dimensional model was simulated and a sensitivity analysis was conducted. For carbonate reservoirs with the presence of interlayer, the average oil production rate decreased by 8% after 2 years; however, the numerical simulation results show that the average oil production rate returned to within 5% after 8 years of production. It may be due to the presence of interlayer and lateral expansion of the steam chamber. The simulation results are basically consistent with the conclusions of Yang and Butler. All the above simulations are based on the assumptions that there lie thin interlayers in a two-dimensional model and the simulation results are quite restrictive. In 2008, Q. Chen [27] conducted a numerical study on the effect of reservoir heterogeneity on the production of SAGD flooding. The inverted triangle steam chamber was divided into two parts, namely, the near-wellbore area (NWR) and the above-wellbore area (AWR). Subsequent research results show that the division of the near-wellbore and above-wellbore zones is significant in decoupling the complex impact of reservoir heterogeneity on the SAGD process. In 2008, numerical simulation methods were used to evaluate the shale interlayer problem during the SAGD process by G. Ipek [28]. It was further suggested that if the lateral range of shale interlayer is large enough and traverses the lateral reservoir range, the oil recovery is likely to be seriously reduced. The method of increasing reservoir permeability through high-pressure circulation was also proposed to minimize the impact of shale interlayer. However, due to the combined influence of reservoir stress and pressure, strict geomechanical predictions for expansion and fractures were not yet possible at that time. In 2012, S.M. Fatemi [29] conducted numerical simulations to study the effects of different geometric properties of shale interlayers on the production of SAGD flooding and the development degree of steam chambers. The longer the length and higher the density of continuous shale interlayers, the worse the SAGD effect. The smaller the vertical distance between the continuous shale interlayer and the steam injection well, the lower the recovery rate. The distribution of interlayers can also affect oil recovery and production. Grebe and Stoesser [30] found from the observation of experimental phenomena that the injection pressure sometimes exceeds the fracture pressure of the formation when acid is injected, indicating that the reservoir is also fractured during acidizing. This was the first time that reservoir hydraulic fracturing was described in the application of acid treatment technology. Clason [31] pointed out for the first time that it is impossible to increase production through radial infiltration (matrix treatment) of acid in the observations of acidizing treatment of carbonate rocks. It is believed that, as the presence of cracks, the significant increase in productivity can only be explained by expanding the cracks and removing drilling fluid or other sediment from the cracks or fractures. About a decade after it was first proposed, this viewpoint could be confirmed. Another important milestone in the researching field of acid fracturing was in 1972, when Nierode and Williams [32] proposed a kinetic model for the reaction between hydrochloric acid and limestone. The model can be used to predict the acid reaction during the fracturing process and design an acidizing fracturing plan. The emergence of this model transformed carbonate rock acidification from a mysterious problem to a scientific study that can be predicted. In 1989, Jennings [33] first used acid fracturing technology in sandstone reservoirs and applied for a patent. The process is divided into several steps. The pad fluid is gelled foam acid. After the injection of pad fluid for fracturing and creating cracks, ungelled foam acid was subsequently injected to form finger in the gelled foam acid, resulting in the formation of a rough acid-etching fracture surface. The secondary damage caused by acidification in sandstone reservoirs [34] is very severe, and hence, the selection of acid solution is extremely important.

Previous studies have focused on the effects of the hinderance of low-permeability interlayers on steam chamber expansion and production in the SAGD development of reservoirs. It has been proposed that both supplementing perforations for steam injection above low-permeability interlayers and optimizing well patterns are effective means to

ensure productivity when SAGD flooding is applied to the combination of vertical and horizontal wells [35]. There are currently some means to break through low-permeability interlayers. Nevertheless, these means cannot meet the dual needs of economic benefits and development effects at the same time. Acidizing fracturing, as a commonly used method for increasing production and permeability in low-permeability reservoirs in oil fields, has a history of nearly a century and the technology is relatively mature. However, there is no practical application of acidizing fracturing technology in combination with SAGD development to break through low-permeability interlayers.

In this paper, based on the actual situation of different well types in China (including vertical wells, horizontal wells, multistage fracturing wells and so on), the application of acidizing fracturing-assisted SAGD development was especially studied. For reservoirs with low-permeability interlayers that affect production, targeted acidizing fracturing was applied to achieve permeability enhancement, ultimately enabling the steam chamber to break through the interlayers smoothly and quickly. The working fluids systems suitable for different blocks during targeted acidizing fracturing were constructed and the crack parameters were optimized. The application of the combination of targeted acidizing fracturing and SAGD flooding was proposed for improving oil production and reducing the distribution of remaining oil in the development reservoir, which has a high reference value for on-site production.

2. Experimental Section

2.1. Acid Sensitivity Experiment of Rocks in Intervals with Low Physical Properties

The main components of the reservoir sandstones measured via X-ray powder diffraction (XRD) technology are volcanic rock debris (42.1%), quartz (15.3%) and feldspar (13.5%) [36]. The complex matrix mainly includes argillaceous (8.4%) and kaolinite (2.2%). The cement is mainly calcite (2.8%), and the cementation type containing trace siderite is mainly pore type, as shown in Figure 3.



(a) experimental core 1 (b) experimental core 2 (c) experimental core 3 (d) experimental core 4

Figure 3. Natural core samples.

Natural cores were used to conduct the reservoir acid sensitivity evaluation; the experiments were mainly conducted according to the standards of the oil and gas industry. Four cores from different wells were selected to carry out the acid sensitivity evaluation experiment. The basic data are shown in Table 1.

Table 1. Base data of cores used in acid sensitivity experiment.

Core Number	Length (cm)	Diameter (cm)	Dry Weight (g)	Wet Weight (g)	Pore Volume (cm ³)	Permeability (10 ⁻³ μm ²)
1	7.82	2.512	86.485	92.772	6.292	0.076
2	5.104	2.518	44.33	50.22	5.89	0.083
3	8.44	2.508	93.275	100.21	6.935	0.072
4	5.41	2.49	73.641	79.96	6.319	0.073

2.2. Optimization of Acidizing Formula Systems for Intervals with Low Physical Properties

The main acid components in the acidizing solution were optimized to achieve the best dissolution effect.

2.2.1. Experimental Methods

(1) It was seen from the reservoir characteristics of the low-permeability interlayer in the studied block that the contents of calcrete sandstone, argillaceous siltstone, sandy conglomerate and the carbonate in the mineral composition of the low-permeability interlayer rocks were uncertain. The effect of hydrochloric acid alone on the dissolution of the target reservoir was not good [37,38]. Therefore, it was determined that the three main acids used to prepare the mixed acid should include hydrochloric acid, hydrofluoric acid and fluoborate acid.

(2) Single-acid solution dissolution experiments were conducted to observe the dissolution effect of each acid on the core powder. The approximate range of the amount of each acid was preliminarily determined.

(3) The concentration of each acid was adjusted gradually to compound the acidizing fluid system. Under the premise of achieving the dissolution effect, the economic cost was saved as far as possible, and the final main acid formulations suitable for the corresponding blocks were determined.

2.2.2. Experimental Instruments and Equipment

Totals of 36% hydrochloric acid, 40% hydrofluoric acid and 40% fluoroboric acid were used to prepare the acidizing fluid. A universal crusher, sample screen, thermostat and extraction-type oil washing instrument were used to carry out the experiments. The natural cores were taken from the inspection well in the Shuyi District. The crude oil and formation water were provided by the Shuyi District of Liaohe Oilfield.

2.2.3. Experimental Procedures

(1) The oil of large pieces of cores mentioned in Table 1 was absorbed and these cores were dried, and then the cores were crushed and sifted.

(2) The analytical balance was used to accurately weigh 5 g of core sample, and the weight was recorded as m_1 .

(3) A total of 50 mL acid solution of different mass concentration was measured via a plastic measuring cylinder and then poured into plastic beaker.

(4) The core samples were poured into the acid solution, the solution was stirred with a plastic rod until the sample was all wet and then placed, and the time was recorded.

(5) The mixture of acid and core sample was put into the oven at a temperature of 45 °C, which simulated the actual temperature of the formation of Liaohe Oilfield Shuyi District (Figure 4).

(6) The filter paper was put in the oven and dried at 100 °C for 4 h. The filter paper was weighed as m_f .

(7) After reacting for 4 h, the beaker was taken out and the solution was filtered. The filtrate was rinsed with ultra-pure water until it was neutral (Figure 5).

(8) The residual sample together with filter paper was put into a drying oven of 45 °C until the weight was constant.

(9) The total mass of filter paper and the residual sample was weighed and recorded as m_2 , and then the dissolution rate was calculated with the following equation [39].

$$\Delta m = m_2 - m_f \quad (1)$$

$$dissolution\ rate = \frac{(m_1 - \Delta m)}{m_1} \times 100\% \quad (2)$$

where m_2 was the mass of filter paper after the reaction, g, and m_1 was the initial mass of the core, g.

The type and concentration of acid solution were changed successively, and the corresponding dissolution rates were calculated and recorded.



Figure 4. Core powder dissolution experiment. (a) Experimental core 1; (b) experimental core 2; (c) experimental core 3; (d) experimental core 4.

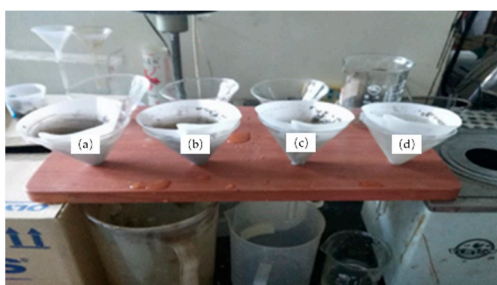


Figure 5. Residue filtration. (a) Experimental core 1; (b) experimental core 2; (c) experimental core 3; (d) experimental core 4.

2.3. Acidizing for Permeability Enhancement Experiment of Rocks in Intervals with Low Physical Properties

(1) The experimental devices were connected, as shown in Figure 6.

(2) The core saturated with formation water was put into the device, and the simulated formation water was injected into the core at a flow rate of 0.30 mL/min. After the flow state became stable, the original permeability K_1 of the core was calculated. The base data of cores used in permeability enhancement experiment are shown in Table 2.

(3) A total of 1.0 pore volume (PV) of acidizing solution was injected into the core, and then the core was placed in a 98 °C incubator for 24 h.

(4) The formation water was subsequently injected into the core with the same flow rate of 0.30 mL/min. After the flow state became stable, the permeability K_2 after acidizing was calculated.

The permeability enhancement rate S was calculated with the following equation.

$$S = (K_2 - K_1) / K_1 \quad (3)$$

Table 2. Base data of cores used in permeability enhancement experiment.

Core Number	Length (cm)	Diameter (cm)	Formation Water Viscosity (mPa·s)	Dry Weight (g)	Wet Weight (g)	Pore Volume (cm ³)	Flow Rate (mL/min)
1	5.41	2.49	0.5	62.34	71.59	9.25	0.30
2	7.17	2.51	0.5	64.28	72.80	8.52	0.30
3	6.32	2.50	0.5	63.95	72.81	8.86	0.30
4	5.86	2.49	0.5	63.51	72.64	9.13	0.30

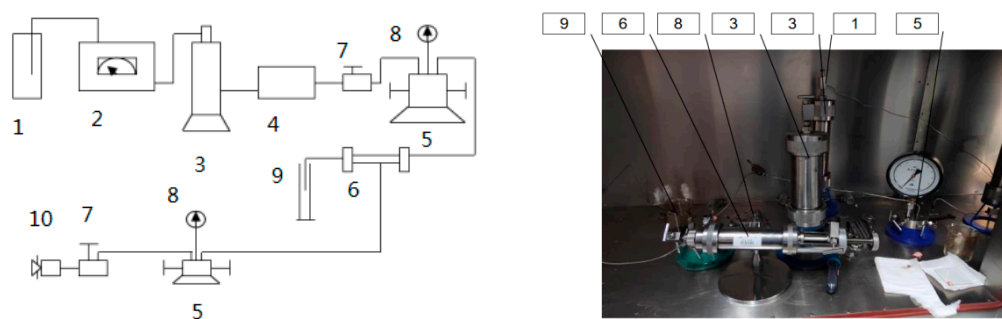


Figure 6. Schematic diagram of the acidizing displacement experimental setup. 1—Liquid bottle; 2—constant speed pump; 3—intermediate container; 4—filter; 5—way valve; 6—core gripper; 7—regulating valve; 8—pressure gauge; 9—measuring cylinder; 10—manual pressure pump.

3. Results and Discussion

3.1. Basic Characteristics of Low Physical Intervals Developed by SAGD Method

Four cores from different wells were selected to carry out the acid sensitivity evaluation experiments. It was seen from the experimental results, shown in Table 3, that the target formation was highly acid-sensitive. Attention should be paid to the strict control of the acidity of the working fluid, and an appropriate corrosion inhibitor and acid residue inhibitor should be added.

Table 3. Acid sensitivity experiment results.

Core Number	K'_f ($10^{-3} \mu\text{m}^2$)	K_{ad} ($10^{-3} \mu\text{m}^2$)	Acid Sensitivity Index I_a (%)	Level of Sensitivity
1	0.076	0.025	65.5	pole-strength
2	0.083	0.034	65.41	pole-strength
3	0.072	0.033	67.12	pole-strength
4	0.073	0.028	56.31	pole-strength

The measurement results of rock and mineral composition are shown in Table 4. The minerals in the intervals with low physical properties of this well developed with SAGD flooding were mainly siderite. The results of the acid sensitivity evaluation showed that the acid sensitivity index of this well was large, indicating that fluoroborate or hydrofluoric acid had a better acidizing effect. However, the acid content should not be too high; excessive acidizing might lead to collapse of the formation.

Table 4. Mineral composition of rocks.

Core Number	Quartz	Potash Feldspar	Plagioclase	Calcite	Ankerite	Dolomite	Siderite	Pyrite	Clay Mineral
1	52.4	25.4	18.0	0.2	1.1	-	-	-	2.8
2	32.4	19.1	29.7	-	-	1.8	16.2	-	0.8
3	22.5	20.5	42.0	-	-	-	9.7	-	5.2
4	17.6	14.3	16.7	-	-	-	44.0	-	7.4

Electron microscope images of the core before acidizing are shown in Figure 7. It was observed that the particles before acidizing were large and the mineral composition contained in the core was relatively abundant. Provided that the selected acidizing fluid did not match the minerals present in the reservoir or inevitably reacted with them, it would be easy to cause formation blockage and some difficulties. Therefore, it was necessary to consider how to improve the structure and porosity of rock under the action of acidifiers and increase the seepage capacity of fluid when optimizing the formulation of an acidizing fluid system, so as to enhance oil recovery.

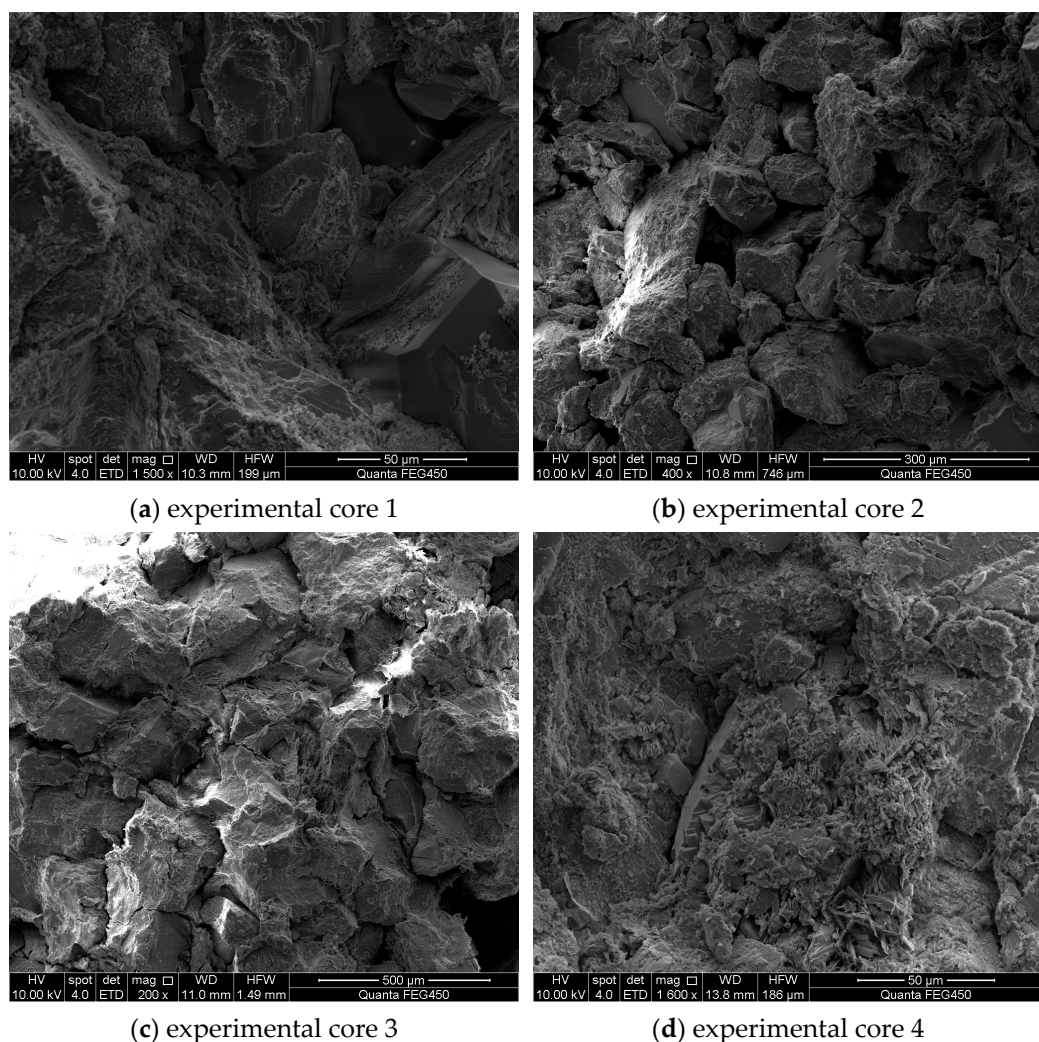


Figure 7. Electron microscope images of the core before acidizing.

3.2. Optimization of Acidizing Formula System for Low Physical Property Intervals

Firstly, a variety of single-component acid solutions was used for dissolution experiments. Single hydrochloric acid with a concentration of 5–13%, single hydrofluoric acid with a concentration of 1–5% and single fluoboric acid with a concentration of 1–7% were prepared according to the field experience in Liaohe Oilfield Shuyi District. The dissolution effects of them within 4 h were tested, respectively. It could be seen from the experimental results shown in Figure 8 that the highest dissolution rate produced by a single hydrochloric acid solution was 14.02%. As a result, the conclusion that the content of carbonate in the core was not much was drawn. Both the dissolution rates of hydrofluoric acid and fluoroborate acid were higher than that of hydrochloric acid, which could reach 39.18% and 31.02%, respectively.

The three main acids used to prepare the mixed acid include hydrochloric acid, hydrofluoric acid and fluoborate acid. Hydrochloric acid costs less; however, the dissolution effect of single hydrochloric acid is not good. The high-cost fluoroborate or hydrofluoric acids have better acidizing effects due to the large acid sensitivity index of the targeted sections. Therefore, when compounding these three types of acid, increasing the amount of fluoroborate and hydrofluoric acid can achieve better acidizing and dissolution effects, while increasing the proportion of hydrochloric acid in the whole system as much as possible under the condition of ensuring the effect is beneficial can save cost. Then, these three acids were mixed to prepare the acidizing formula system; during this period, it was necessary to ensure that the various components in the core were fully dissolved. The

concentrations of each acid were determined in turn via a single-variable method. When optimizing the concentration of fluoboric acid, the concentration of hydrochloric acid was set as 8% and that of hydrofluoric acid was set as 2% tentatively. The concentration of fluoroborate acid was adjusted to observe whether the dissolution rate was close to the ideal value. As seen from the experimental results in Figure 9, the dissolution rate obtained at this concentration ratio was too high.

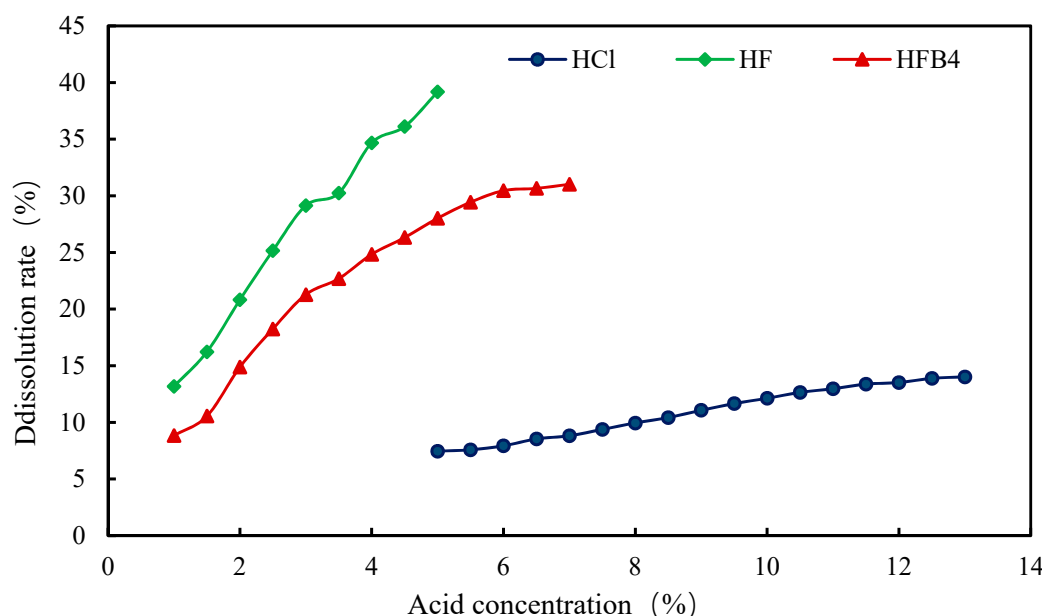


Figure 8. Change in core dissolution rate with concentration of a single-acid solution.

Therefore, the concentrations of hydrochloric acid and hydrofluoric acid must be adjusted. When the concentration of hydrofluoric acid was set as 7% and the concentration of hydrofluoric acid was unchanged (2%), the dissolution rates were lower than the previous results by adjusting the concentration of fluoboric acid. In this case, the dissolution rate was still slightly higher than expected, which may be due to the high concentration of hydrofluoric acid. Then, the change in dissolution rate with the concentration of fluoboric acid when the concentration of hydrofluoric acid was set at 1.5% and the concentration of hydrochloric acid was 7% was measured. The dissolution rate under this acid ratio tended to the ideal value, while it still needed further adjustment.

Afterwards, the concentration of hydrochloric acid was set as 5% and the concentration of hydrofluoric acid was 1%, so that the concentration of fluoboric acid was further optimized. As seen from Figure 9, the best dissolution effect could be achieved when the concentration of fluoboric acid was 3%. Due to the high cost of using fluoboric acid, the concentration of fluoboric acid was set at 3% for economic consideration.

Then, the concentration of hydrochloric acid was optimized when the concentration of fluoboric acid was fixed at 3%. It can be seen from Figure 10 that when the concentration of hydrofluoric acid was set as 2%, no matter how the concentration of hydrochloric acid was adjusted, the dissolution rate was always relatively high. As a result, the concentration of hydrofluoric acid was reduced to 1%, and the dissolution rate could gradually tend to the ideal value.

In order to slow down the rate and prevent iron ion precipitation, 1% acetic acid was added to the formula, and the concentration of hydrochloric acid was adjusted to observe the change in dissolution rate. As seen in Figure 10, when the concentration of fluoboric acid was 3% and the concentration of hydrofluoric acid was 1%, a good dissolution effect could be obtained at 7% concentration of hydrochloric acid. As the concentration of hydrochloric acid continued to increase, the dissolution rate increased slightly. At the same time, corrosion inhibitors needed to be added to meet the requirements of anticorrosion.

From an economic point of view, the concentration of hydrochloric acid was determined to be 7%.

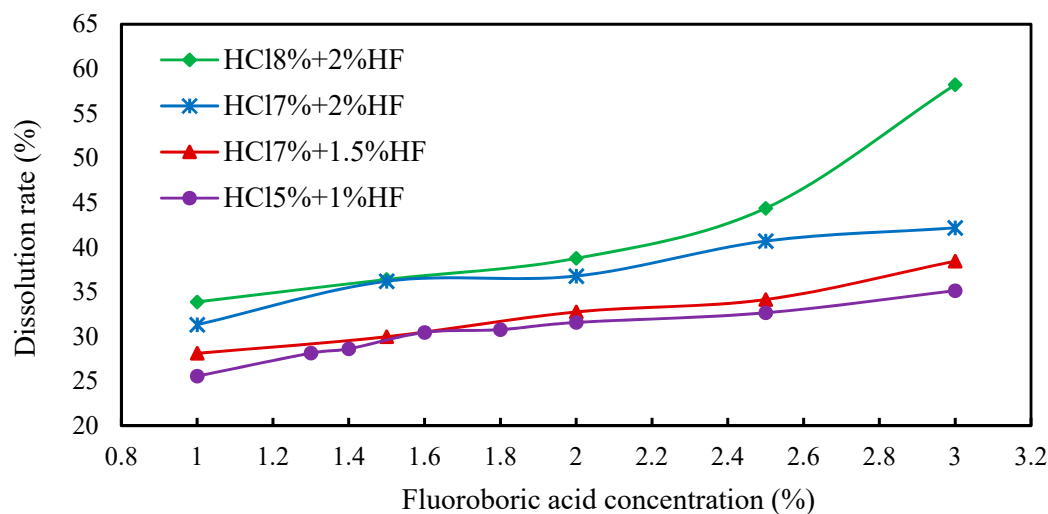


Figure 9. Dissolution rate curve of fluoboric acid solution under different acid ratios.

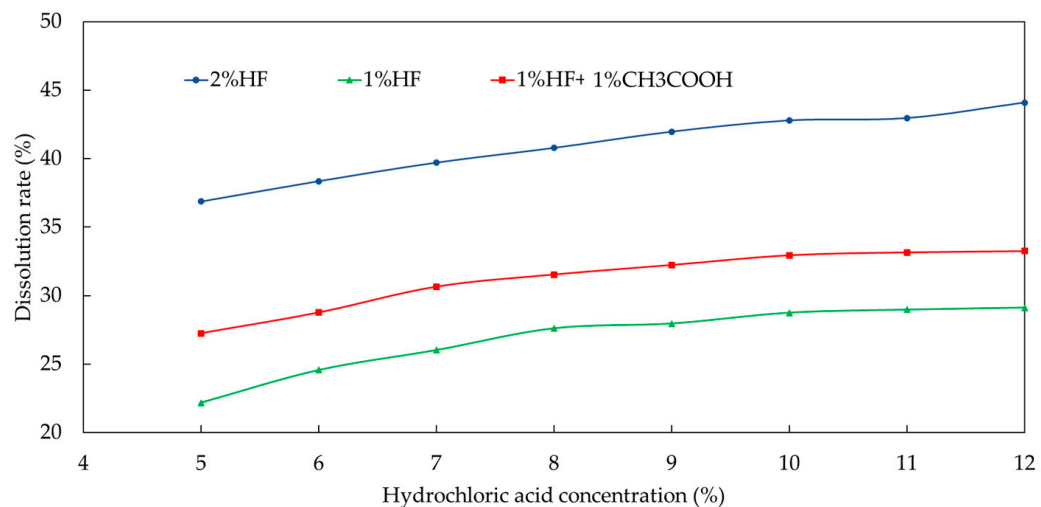


Figure 10. Effect of concentration of hydrochloric acid on dissolution rate.

Then, the concentration of hydrofluoric acid was optimized under the condition that the concentrations of fluoboric acid and hydrochloric acid were set as 3% and 7%, respectively. It can be observed from Figure 11 that the dissolution rate was 37.36% when the concentration of hydrofluoric acid was 2.5%. As the concentration of hydrofluoric acid continued to increase, the dissolution rate did not increase significantly. Consequently, the concentration of hydrofluoric acid was determined to be 2.5%.

Based on the above experimental results, 1% acetic acid should be added to the acid system as the retarding acid solution to maintain the pH of the acid solution to a certain extent and prevent the formation of secondary precipitation. Meanwhile, acetic acid played the role of chelating iron ions and retarding. Therefore, the main acid formula of '7% hydrochloric acid + 3% fluoboric acid + 2.5% hydrofluoric acid + 1% acetic acid' was obtained.

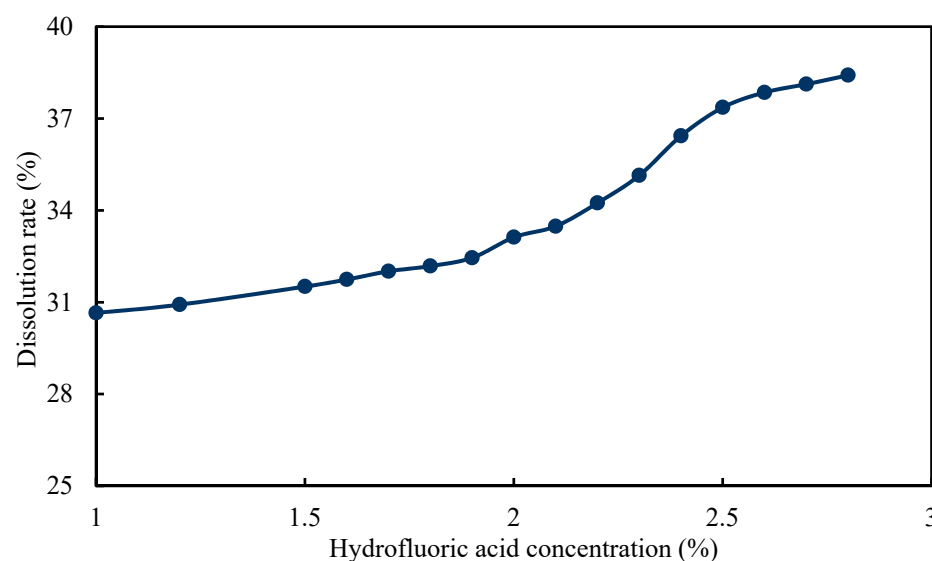


Figure 11. Dissolution rate curve of hydrofluoric acid solution with different concentration.

3.3. Permeability Enhancement Effect Achieved by Acidizing the Intervals with Low Physical Properties of Wells Developed by SAGD Method

The dissolution effects of various acids were observed using core slice dissolution experiments. The core slices were soaked in different solutions at 45 °C for 4 h. The changes in the slices before and after the experiment were compared. Considering the strong acid sensitivity of the reservoir, a certain amount of ethanol was added to the main acid for regulation. A total of eight solution combinations, as shown in Table 5, were selected to carry out the experiment.

Table 5. Solution combinations used in core slice dissolution experiments.

Number	Formular
1	Formation water + 2% ethanol
2	Distilled water + 2% ethanol
3	10% hydrochloric acid + 2% ethanol
4	5% hydrofluoric acid + 2% ethanol
5	5% fluoroboric acid + 2% ethanol
6	5% polyphosphate + 2% ethanol
7	3% polyphosphate + 2% fluoroboric acid
8	4% hydrochloric acid + 2% polyphosphate + 5% fluoroboric acid + 4% acetic acid + 2% ethanol

A polarizing microscope was used to observe the micromorphologies of core slices before and after acidizing. As shown in Figure 12, hydrochloric acid and polyphosphate had poor dissolution effects on target formation. The dissolution effects caused by hydrofluoric acid and fluoroboric acid were relatively good (especially fluoroboric acid); however, the pores after dissolution were likely to be blocked by small particles. The combination of the above multiple-acid solutions could effectively address the problem of particle migration, thereby improving the permeability enhancement ability. Consequently, the acid solution formula was adjusted to be ‘4% hydrochloric acid + 2% polyphosphate + 5% fluoroboric acid + 4% acetic acid + 2% ethanol’.

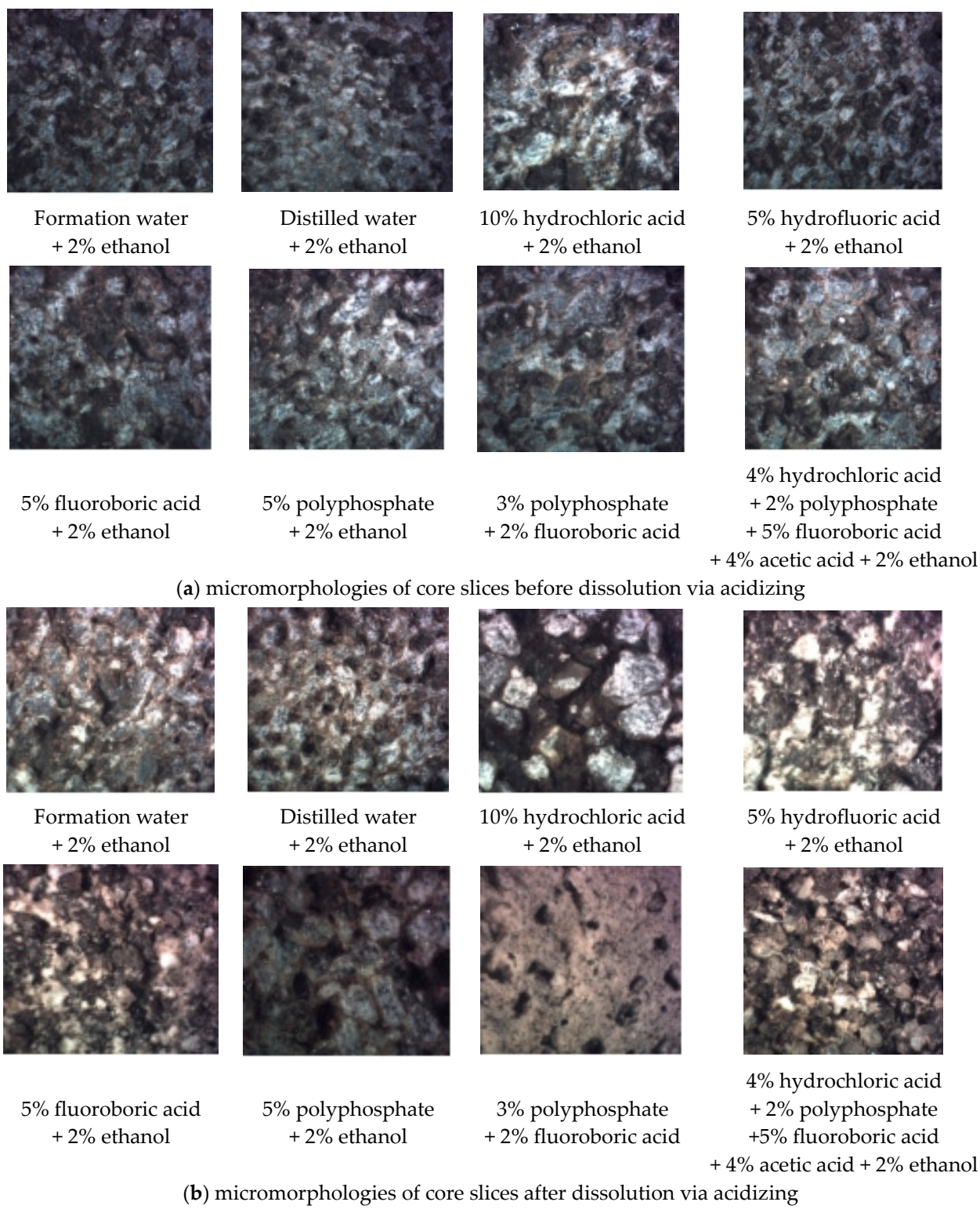


Figure 12. Core slices observed via polarizing microscope (magnification times 200).

The adjusted acid solution was used for the acidizing and permeability enhancement experiment. It can be seen from the displacing evaluation shown in Figure 13 that the permeability increase range was between 35.48% and 57.06%. Hence, the conclusion that the acid fracturing working fluid formula had a good acidizing and permeability enhancement effect on natural cores was fully verified, which could meet the requirements of construction.

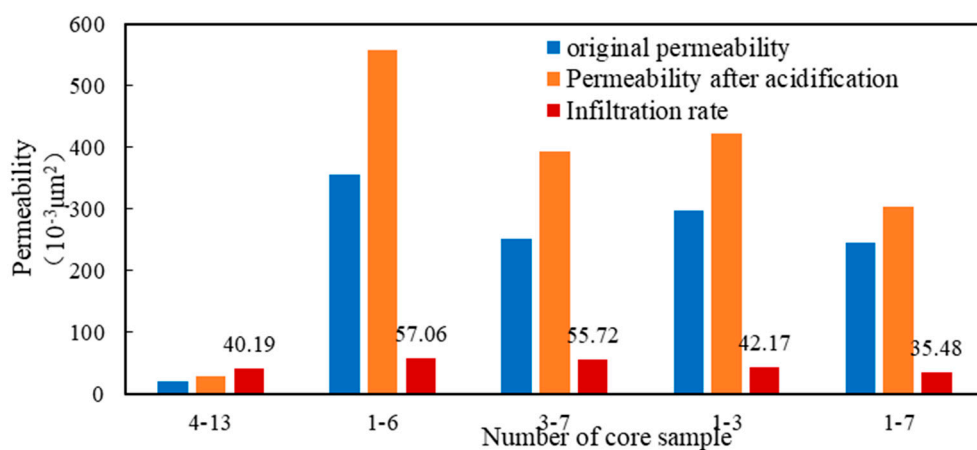


Figure 13. Enhanced permeability experimental result of different cores.

According to the optimized acid fluid formula system in Figure 13, on-site experiments were conducted on acid fracturing. The experimental block was the oil well of SAGD in the Shuguang Oil Production Plant of Liaohe Oilfield. As shown in Figure 14, the initial daily increase in oil production was 1.6 t. So far, a cumulative oil production increase of 1002 t has been achieved in this district.

After the combination of acidizing fracturing and SAGD flooding was applied, the water cut decreased and the oil production increased obviously. Therefore, it could be concluded that acidizing fracturing in intervals with poor physical properties of steam-assisted gravity enhanced reservoir permeability, thus effectively improving oil recovery.

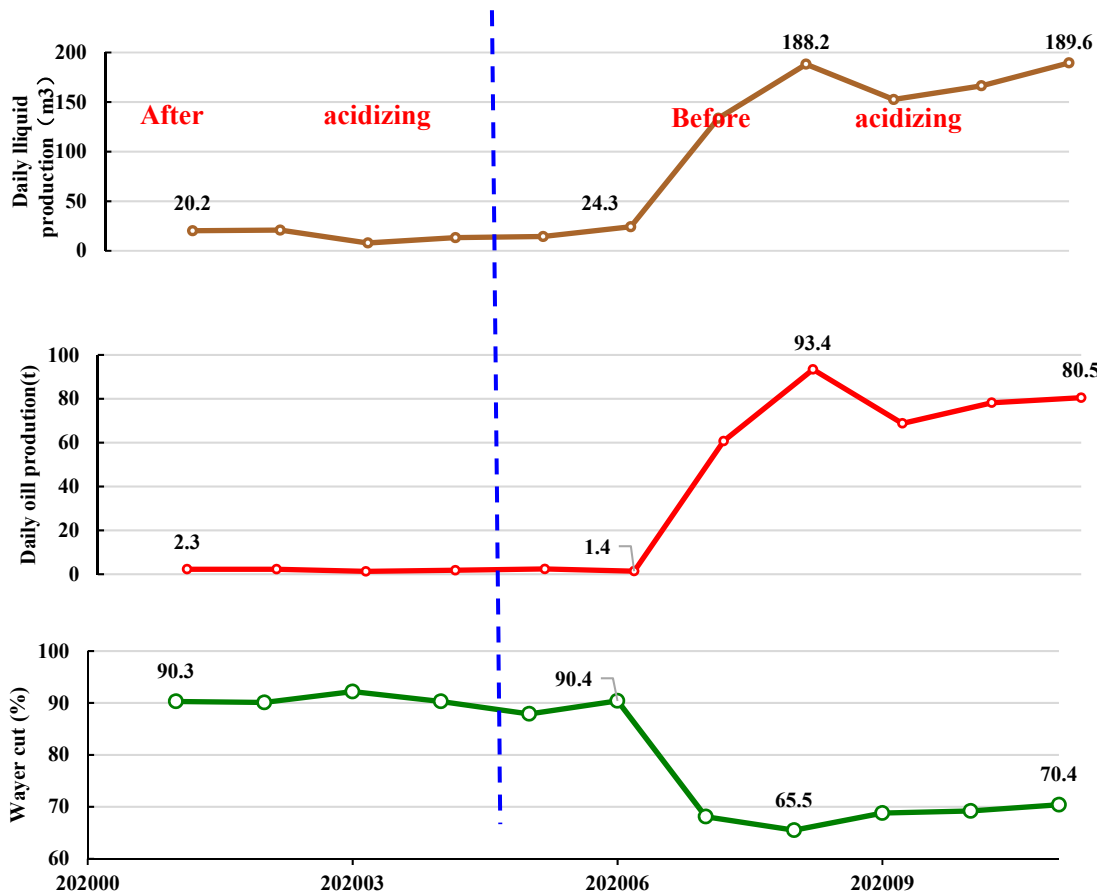


Figure 14. Production curves of S₁₋₁₋₅ wells in Shuyi District of Liaohe Oilfield in China.

4. Conclusions

Combining targeted acidizing fracturing and SAGD flooding is an effective method of breaking through low-permeability interlayers, enabling the steam chamber to break through interlayers smoothly and quickly. In this paper, the acid fracturing working fluid suitable for Liaohe Oilfield Shuyi District was determined.

- (1) The results of core dissolution experiments showed that hydrochloric acid and polyphosphate had poor dissolution effects on the formation. Although hydrofluoric acid and fluoroboric acid, especially fluoroboric acid, had good dissolution effects, they were prone to form small particles that plugged pores after dissolution.
- (2) The combination of multiple acids can effectively address the problem of particle migration, thereby improving the permeability enhancement ability. The actual permeability-enhancing capacity of the acid fracturing working fluid formula '4% hydrochloric acid + 2% polyphosphate + 5% fluoroboric acid + 4% acetic acid + 2% ethanol' was verified with the natural core of the corresponding block.
- (3) Acidizing measures implemented on-site led to the beginning of a reduction in water cut and increase in oil production, indicating that applying acidizing could enhance permeability. The range of enhancement permeability of the acidizing system in intervals with low physical properties of the reservoir developed via SAGD flooding was 35.48%~57.06%.

Author Contributions: Conceptualization, M.Y.; Methodology, C.X.; Validation, C.X.; Formal analysis, Y.B.; Investigation, Y.B., C.Z. and J.Z.; Resources, X.Y.; Writing—original draft, M.Y.; Writing—review & editing, G.C.; Visualization, W.L. All authors have read and agreed to the published version of the manuscript.

Funding: This research was funded by [the National Natural Science Foundation of China] grant number [No. 51574089].

Data Availability Statement: The data is unavailable due to privacy.

Conflicts of Interest: The authors declare no conflict of interest.

References

1. Ugursal, A.; Zhu, D.; Hill, A.D. Development of Acid Fracturing Model for Naturally Fractured Reservoirs. *SPE Prod. Oper.* **2019**, *34*, 735–748. [[CrossRef](#)]
2. Chen, X.; Luo, Z.; Zhao, L.; Xiong, X.; Chen, W.; Miao, W.; Zhang, N.; Chen, X. Hydraulic, acid, and proppant-carrying acid fracturing stimulation of volcanic reservoirs in Sichuan Basin, China: An experimental study. *Pet. Sci. Technol.* **2023**, *41*, 731–749. [[CrossRef](#)]
3. Lin, H.; Hou, T.; Wang, F.; Yue, L.; Liu, S.; Yuan, G.; Wang, G.; Liu, Y.; Wang, Q.; Zhou, F. Experimental Study of Acid Etching and Conductivity of High-Temperature-Resistant Cross-Linked Acid. *Processes* **2023**, *11*, 722. [[CrossRef](#)]
4. Al-Bahlani, A.M.; Babadagli, T. SAGD laboratory experimental and numerical simulation studies: A review of current status and future issues. *J. Pet. Sci. Eng.* **2009**, *68*, 135–150. [[CrossRef](#)]
5. Butler, R.M.; Mcnab, G.S.; Lo, H.Y. Theoretical studies on the gravity drainage of heavy oil during in-situ steam heating. *Can. J. Chem. Eng.* **1981**, *59*, 455–460. [[CrossRef](#)]
6. Cheng, Q.; Cao, G.; Bai, Y.; Zhu, Z.; Zhang, Z.; Li, D. Probing the Demulsification Mechanism of Emulsion with SPAN Series Based on the Effect of Solid Phase Particles. *Molecules* **2023**, *28*, 3261. [[CrossRef](#)]
7. Shin, H.; Polikar, M. Optimizing the SAGD Process in Three Major Canadian Oil-Sands Areas. In Proceedings of the SPE Annual Technical Conference and Exhibition, Dallas, TX, USA, 9–12 October 2005.
8. Polikar, M.; Cyr, T.J.; Coates, R.M. Fast-SAGD: Half the Wells and 30% Less Steam. In Proceedings of the SPE/CIM International Conference on Horizontal Well Technology, Calgary, AB, Canada, 6–8 November 2000.
9. Shin, H.; Polikar, M. Review of Reservoir Parameters to Optimize SAGD and Fast-SAGD Operating Conditions. *J. Can. Pet. Technol.* **2007**, *46*, 35–41. [[CrossRef](#)]
10. Ito, Y.; Suzuki, S. Numerical Simulation of the SAGD Process in the Hangingstone Oil Sands Reservoir. *Can. Pet. Technol.* **1999**, *38*, 27–35. [[CrossRef](#)]
11. Ito, Y.; Ipek, G. Steam-Fingering Phenomenon During SAGD Process. In Proceedings of the SPE International Thermal Operations and Heavy Oil Symposium, Calgary, AB, Canada, 1–3 November 2005.
12. Gates, I.D.; Chakrabarty, N. Optimization of Steam Assisted Gravity Drainage in McMurray Reservoir. *Can. Pet. Technol.* **2006**, *45*, 54–62. [[CrossRef](#)]

13. Gates, I.D.; Kenny, J.; Hernandez-Hdez, I.L.; Bunio, G.L. Steam-Injection Strategy and Energetics of Steam-Assisted Gravity Drainage. *SPE Res. Eval. Eng.* **2007**, *10*, 19–34. [[CrossRef](#)]
14. Sharma, J.; Gates, I.D. Multiphase flow at the edge of a steam chamber. *Can. J. Chem. Eng.* **2010**, *88*, 312–321. [[CrossRef](#)]
15. Mou, J.; He, J.; Zheng, H.; Zhang, R.; Zhang, L.; Gao, B. A New Model of Temperature Field Accounting for Acid–Rock Reaction in Acid Fracturing in Shunbei Oilfield. *Processes* **2023**, *11*, 294. [[CrossRef](#)]
16. Jiang, T.; Wang, H.; Bian, X.; Wang, D.; Zhou, J.; Yu, B. Numerical Simulation on Hydrofracture Propagation in Fractured-Vuggy Unconventional Reservoirs. *Geofluids* **2022**, *2022*, 1453–1467. [[CrossRef](#)]
17. Wang, Y.; Yang, J.; Wang, T.; Hu, Q.; Lv, Z.; He, T. Visualization experiment of multi-stage alternating injection acid fracturing. *Energy Rep.* **2022**, *8*, 9094–9103. [[CrossRef](#)]
18. Sui, Y.; Cao, G.; Guo, T.; Li, Z.; Bai, Y.; Li, D.; Zhang, Z. Development of gelled acid system in high-temperature carbonate reservoirs. *J. Pet. Sci. Eng.* **2022**, *216*, 110836. [[CrossRef](#)]
19. Zhao, H.; Xiong, Y.; Zhen, H.; Liu, C.; Li, X. Experimental investigation on the fracture propagation of three-stage acid fracturing of tight sandstone gas reservoir. *J. Pet. Sci. Eng.* **2022**, *211*, 110143. [[CrossRef](#)]
20. Mehrjoo, H.; Norouzi-Apourvari, S.; Jalalifar, H.; Shahari, M. Experimental study and modeling of final fracture conductivity during acid fracturing. *J. Pet. Sci. Eng.* **2022**, *208*, 109192. [[CrossRef](#)]
21. Dou, H.; Xie, J.; Xie, J.; Sun, G.; Li, Z.; Wang, Z.; Miao, Y. Study on the mechanism of the influence of HNO_3 and HF acid treatment on the CO_2 adsorption and desorption characteristics of coal. *Fuel* **2022**, *309*, 122187. [[CrossRef](#)]
22. Yan, F.; Shi, Y.; Tian, Y. Synthesis and Characterization of Surfactant for Retarding Acid–Rock Reaction Rate in Acid Fracturing. *Front. Chem.* **2021**, *9*, 715009. [[CrossRef](#)]
23. Xu, H.; Cheng, J.; Zhao, Z.; Lin, T.; Liu, G.; Chen, S. Coupled thermo-hydro-mechanical-chemical modeling on acid fracturing in carbonatite geothermal reservoirs containing a heterogeneous fracture. *Renew. Energy* **2021**, *172*, 145–157. [[CrossRef](#)]
24. Gou, B.; Zhan, L.; Guo, J.; Zhang, R.; Zhou, C.; Wu, L.; Ye, J.; Zeng, J. Effect of different types of stimulation fluids on fracture propagation behavior in naturally fractured carbonate rock through CT scan. *J. Pet. Sci. Eng.* **2021**, *201*, 108529. [[CrossRef](#)]
25. Zhang, Y.; Zheng, Y.; Jiang, B.; Yu, G.; Ren, B.; Yu, C.; Wang, S. Experimental study on the influence of acid fracturing fluid on coal wettability. *Fuel* **2023**, *343*, 127965. [[CrossRef](#)]
26. Yang, G.; Butler, R.M. Effects of reservoir heterogeneities on heavy oil recovery by steam-assisted gravity drainage. *J. Can. Pet. Technol.* **1990**, *31*, 37–43. [[CrossRef](#)]
27. Kisman, K.E.; Yeung, K.C. Numerical Study of the SAGD Process in the Burnt Lake Oil Sands Lease. In Proceedings of the SPE International Heavy Oil Symposium, Calgary, AB, Canada, 19–21 June 1995.
28. Chen, Q.; Gerritsen, M.G.; Kovscek, A.R. Effects of Reservoir Heterogeneities on the Steam-Assisted Gravity-Drainage Process. *SPE Res. Eval. Eng.* **2008**, *11*, 921–932. [[CrossRef](#)]
29. Ipek, G.; Frauenfeld, T.; Yuan, J.Y. Numerical Study of Shale Issues in SAGD. In Proceedings of the Canadian International Petroleum Conference, Calgary, AB, Canada, 17–19 June 2008.
30. Fatemi, S.M. The Effect of Geometrical Properties of Reservoir Shale Barriers on the Performance of Steam-assisted Gravity Drainage (SAGD). *Energy Sources Part A Recovery Util. Environ. Eff.* **2012**, *23*, 2178–2191. [[CrossRef](#)]
31. Lo, K.K.; Dean, R.H. Modeling of Acid Fracturing. *SPE Prod. Eng.* **1989**, *4*, 194–200. [[CrossRef](#)]
32. Oeth, C.V.; Hill, A.D.; Zhu, D. Acid Fracturing: Fully 3D Simulation and Performance Prediction. In Proceedings of the SPE Hydraulic Fracturing Technology Conference, The Woodlands, TX, USA, 4–6 February 2013.
33. Williams, B.B.; Nierode, D.E. Design of Acid Fracturing Treatments. *J. Pet. Technol.* **1972**, *24*, 849–859. [[CrossRef](#)]
34. Crowe, C.W.; Hutchinson, B.H.; Trittipo, B.L. Fluid-Loss Control: The Key to Successful Acid Fracturing. *SPE Prod. Eng.* **1989**, *4*, 215–220. [[CrossRef](#)]
35. Zhang, Q.; Liu, P.; Xiong, Y.; Du, J. Self-Generated Organic Acid System for Acid Fracturing in an Ultrahigh-Temperature Carbonate Reservoir. *ACS Omega* **2023**, *8*, 12019–12027. [[CrossRef](#)]
36. Li, C.; Song, L.; Cao, Y.; Zhao, S.; Liu, H.; Yang, C.; Cheng, H.; Jia, D. Investigating the Mechanical Property and Enhanced Mechanism of Modified Pisha Sandstone Geopolymer via Ion Exchange Solidification. *Gels* **2022**, *8*, 300. [[CrossRef](#)]
37. Ryu, M.; Kim, H.; Lim, M.; You, K.; Ahn, J. Comparison of Dissolution and Surface Reactions Between Calcite and Aragonite in L-Glutamic and L-Aspartic Acid Solutions. *Molecules* **2010**, *15*, 258–269. [[CrossRef](#)] [[PubMed](#)]
38. Shan, G.; Igarashi, K.; Ooshima, H. Dissolution kinetics of crystals in suspension and its application to L-aspartic acid crystals. *Chem. Eng. J.* **2002**, *88*, 53–58. [[CrossRef](#)]
39. Ling, D.; Zhu, S.; Zheng, J.; Xu, Z.; Zhao, Y.; Chen, L.; Shi, X.; Li, J. A simulation method for the dissolution construction of salt cavern energy storage with the interface angle considered. *Energy* **2023**, *263*, 125792. [[CrossRef](#)]

Disclaimer/Publisher’s Note: The statements, opinions and data contained in all publications are solely those of the individual author(s) and contributor(s) and not of MDPI and/or the editor(s). MDPI and/or the editor(s) disclaim responsibility for any injury to people or property resulting from any ideas, methods, instructions or products referred to in the content.